

A Fundamental Study of Erosion and Channelization in Debris Flows Using a Shallow Water SPH Approach

Nilo Dolojan ¹⁾, Reika Nomura ²⁾, Kenjiro Terada ³⁾, Shuji Moriguchi ⁴⁾

¹⁾Ph.D. Postdoc Research Fellow, IRIDeS, Tohoku University
(Email: njdolojan@tohoku.ac.jp)

²⁾Ph.D. Assistant Professor, IRIDeS, Tohoku University

³⁾Ph.D. Professor, Dept. of Civil and Environmental Eng, Tohoku University

⁴⁾Ph.D. Associate Professor, IRIDeS, Tohoku University

Erosion and entrainment are crucial factors influencing debris flow hazard volume, runout distance, and severity. However, these complex phenomena remain a challenge to incorporate and characterize in many numerical models. This study investigates this problem by applying a depth-integrated shallow water debris flow model, specifically incorporating a physically-based entrainment formulation derived from mass and momentum balance principles. The model is solved using the mesh-free Smoothed Particle Hydrodynamics (SPH) method allowing for simulation of debris flows over erodible beds and capturing the interaction between the flow and the bed material.

Key Words : *shallow water equations, debris flow, erosion, SPH*

1. INTRODUCTION

Debris flows are fast-moving mixtures of rocks, water, and soil that pose significant hazards in mountainous and tectonically active regions. Their complex behavior, governed by interactions between fluid and solid phases, large deformations, entrainment of bed materials, and localized interaction with irregular terrain, remain challenging to characterize and model consistently. To address these limitations, theoretical simplifications and assumptions are necessary to develop computationally efficient models capable of capturing the dynamics of debris flow processes. Among these, depth-integrated shallow water equations (SWE) incorporating assumptions such as incompressibility, lithostatic pressure distribution, and negligible vertical accelerations, provide a practical framework for simulating debris flow motion across complex topographies.

Therefore, this study applies a depth-integrated debris flow model based on the SWE, enhanced with a combined frictional-turbulent rheological formulation. Moreover, it adopts a physically-based entrainment model derived from the superposition of the mass and momentum balance equations. The governing equations are then reformulated in Lagrangian form and solved using the Smoothed Particle Hydrodynamics (SPH) method, which enables mesh-free simulation of debris flow bodies over large and expansive computational domains. The model is initially applied to replicate the debris flow flume experiments, and is validated against observed flow front positions. Following this validation, the model is extended to simulate debris flow propagation over an erodible bed, capturing entrainment effects and associated volume increases.

2. GOVERNING EQUATIONS

(1) Shallow Water Equations

The depth-integrated SWE are utilized to simulate the dynamic behavior of debris flows. Applying incompressibility, negligible vertical acceleration, and lithostatic pressure assumptions, the continuity and momentum balance considering erosion/entrainment are written as:

$$\frac{\partial \bar{\rho} h}{\partial t} + \frac{\partial \bar{\rho} h \bar{u}}{\partial x} + \frac{\partial \bar{\rho} h \bar{v}}{\partial y} = \bar{\rho} E_b \quad (1)$$

$$\frac{\partial \bar{\rho} h \bar{u}}{\partial t} + \frac{\partial \bar{\rho} h \bar{u}^2}{\partial x} + \frac{\partial \bar{\rho} h \bar{u} \bar{v}}{\partial y} = \bar{\rho} g_x h - k \bar{\rho} g_z h \frac{\partial h}{\partial x} - \tau_{bx} + \bar{\rho} u_b E_b \quad (2)$$

$$\frac{\partial \bar{\rho} h \bar{v}}{\partial t} + \frac{\partial \bar{\rho} h \bar{u} \bar{v}}{\partial x} + \frac{\partial \bar{\rho} h \bar{v}^2}{\partial y} = \bar{\rho} g_y h - k \bar{\rho} g_z h \frac{\partial h}{\partial y} - \tau_{by} + \bar{\rho} v_b E_b \quad (3)$$

where h is the flow height, $\bar{\rho}$, \bar{u} , \bar{v} are the depth-averaged density and velocities, E_b , τ_{bx} , τ_{by} , u_b , v_b are the basal entrainment rate, basal shear stresses, and basal velocities. Here, the variables are expressed in the topography-linked coordinates, with flow height and velocities defined normal and parallel to the slope, respectively.

The lateral earth pressure coefficient k relates the vertical normal stress with the lateral normal stresses, and can be defined using Rankine Theory:

$$\left. \begin{matrix} k_a \\ k_p \end{matrix} \right\} = \frac{1 \mp \sin \phi}{1 \pm \sin \phi} \quad (4)$$

where ϕ is the internal friction angle, and k_a, k_p refers to the active or passive state, corresponding to expansion or compression of the geomaterial.

(2) Rheological Model

To simulate debris flow behavior, the flow resistance or basal shear stress term τ_b must be specified. Particularly, this study employs both the Manning's turbulent model and Coulomb's frictional model defined, respectively, as:

$$\tau_b = \frac{\bar{\rho} g_z n^2 \bar{u} \sqrt{\bar{u}^2 + \bar{v}^2}}{h^{1/3}} \quad (5)$$

$$\tau_b = \bar{\rho} g_z h \cos \alpha \tan \phi \quad (6)$$

where n is the Manning's friction coefficient, α is the slope gradient, and ϕ is the internal friction angle of the material. By modifying only two parameters, n and ϕ , the flow behavior could be modified and calibrated.

(3) Entrainment Model

The entrainment model of debris flow (or erosion from the perspective of the bed surface) is obtained from the superposition of two sets of continuity and momentum equations of the moving debris flow and the static erodible bed. Imposing equilibrium at the boundary of the two layers [1], the basal and surficial stresses and velocities are shown to have the following relationship:

$$E_b = -\frac{\partial z_b}{\partial t} = \frac{\tau_b - \tau_s}{\bar{\rho}(|\mathbf{u}_b| - |\mathbf{u}_s|)} \quad (7)$$

where τ_s, \bar{u}_s are the surface shear resistance and surface velocity of the erodible bed layer. The flow basal shear stress τ_b is the combined turbulent and frictional model defined for the debris flow, while the surface shear resistance τ_s is defined using the Mohr-Coulomb failure criterion of the erodible layer. Assuming the velocity at the surface of the velocity layer to be at rest, the equation can be rewritten as:

$$E_b = \frac{\tau_b - \bar{\rho} g_z h \cos \alpha \tan \phi_s}{\bar{\rho} \sqrt{u_b^2 + v_b^2}} \quad (8)$$

Here, erosion is shown to occur when the flow basal shear stress is larger than the bed surface shear resistance. Additionally, the rate at which erosion occurs increases as the flow basal velocity decreases.

The basal velocity, however, cannot be directly obtained under the shallow water assumption which utilizes depth-averaged velocities. As a simplification, an assumption of a linear velocity profile distribution proposed by Johnson can be applied

$$u_b = (1 - s_1) \bar{u} \quad (9)$$

where s_1 is a fitting parameter from 0 to 1, corresponding to uniform plug flow and shear flow with no basal slip, respectively.

3. NUMERICAL SCHEME

Since debris flows travel over long distances covering wide spatial domains, it is advantageous to discretize the debris flow body as particles, instead of discretizing the entire domain into grids. Therefore, this study employs the mesh-free SPH method to solve the above equations.

(1) Lagrangian Formulation

The governing equations, which are conventionally expressed in the Eulerian formulation, are first rewritten in the Lagrangian form by applying the chain rule and expanding the partial derivatives. The resulting equations are then expressed in terms of the material derivative D/Dt as:

$$\bar{\rho} \frac{Dh}{Dt} + \bar{\rho} h \left(\frac{\partial \bar{u}}{\partial x} + \frac{\partial \bar{v}}{\partial y} \right) + h \frac{D\bar{\rho}}{Dt} = \bar{\rho} E_b \quad (10)$$

$$\bar{\rho} h \frac{D\bar{u}}{Dt} = \bar{\rho} g_x h - k \bar{\rho} g_z h \frac{\partial h}{\partial x} - \tau_{bx} + \bar{\rho} u_b E_b - \bar{\rho} \bar{u} E_b \quad (11)$$

$$\bar{\rho} h \frac{D\bar{v}}{Dt} = \bar{\rho} g_y h - k \bar{\rho} g_z h \frac{\partial h}{\partial y} - \tau_{by} + \bar{\rho} v_b E_b - \bar{\rho} \bar{v} E_b \quad (12)$$

Note the additional term $-\bar{\rho} \bar{u} E_b$ and $-\bar{\rho} \bar{v} E_b$ in the momentum equations, which is not present in the original SWE. This term accounts for the change in velocity due to the entrainment of material from the bed surface, that is expressed implicitly in the inertial terms of the Eulerian SWE.

(2) SPH Discretization

Under the SPH algorithm, the fluid body is discretized into particles each carrying material properties such as density, pressure, velocity, etc. Assuming constant soil density $\bar{\rho}$, the continuity and momentum equations can be discretized as:

$$\frac{Dh_i}{Dt} = -h_i \sum_{j=1}^N \frac{V_j}{h_j} (\mathbf{u}_j - \mathbf{u}_i) \nabla W_{ij} + E_{bi} \quad (13)$$

$$\frac{D\bar{\mathbf{u}}_i}{Dt} = \mathbf{g}_i - k g_z \sum_{j=1}^N \frac{V_j}{h_j} (H_j - H_i) \nabla W_{ij} - \frac{\tau_{bi}}{\rho h_i} + \frac{(\mathbf{u}_{bi} - \bar{\mathbf{u}}_i) E_{bi}}{h_i} \quad (14)$$

Here, the 3D SPH mass m_j , density ρ_j , and volume V_j are analogous to the 2D SWE SPH particle volume V_j , height h_j and area A_j , respectively. Correspondingly, the defined 3D SPH volume $V_j = \rho_j/m_j$ is analogous to the 2D SWE SPH area $A_j = V_j/h_j$.

For simplicity and stability, the gradient term in the momentum equation is redefined as pressure P similar to the 'equation of state' of weakly compressible SPH method.

$$k\bar{\rho}g_z h \frac{\partial h}{\partial x} = \frac{\partial}{\partial x} \left(\frac{1}{2} k\bar{\rho}g_z h^2 \right) = \nabla P \quad (15)$$

and discretized using:

$$\sum_{j=1}^N V_j \left(\frac{P_i}{h_i^2} + \frac{P_j}{h_j^2} + \Pi_{ij} \right) \nabla W_{ij} \quad (16)$$

The artificial viscosity term is used to stabilize and reduce the oscillation in the numerical solution. This paper adopts the artificial viscosity used in the works of Monaghan [2] and Xia [3] as:

$$\Pi_{ij} = - \frac{0.5\nu_{sig} \mathbf{u}_{ij} \cdot \mathbf{r}_{ij}}{\bar{h}_{ij} |\mathbf{r}_{ij}|^2} \quad (17)$$

$$\nu_{sig} = c_i + c_j - 2 \frac{\mathbf{u}_{ij} \cdot \mathbf{r}_{ij}}{|\mathbf{r}_{ij}|^2} \quad (18)$$

where \mathbf{r}_{ij} is the distance vector, $\bar{h}_{ij} = (h_i + h_j)/2$ is the mean flow depth and $c = \sqrt{gh}$ is the wave celerity. These are equivalent with the traditional artificial velocity formulation whose α and β are equal to 1.

4. RESULTS AND DISCUSSION

The model is used to simulate the debris flow experiments of Iverson et al. [4]. The experiment involves the release of a debris flow-like mixture of soil and water with a total volume of 11.78 m³ and wet bulk density of 2,100 kg/m³ over a rectangular concrete channel 95 m long, 2 m wide, and 1.2 m deep (**Fig. 1**). The propagation of the flow front after release is measured and plotted with time. Moreover, sensors measuring the flow height are placed at 32 m (sensor 1) and 66 m (sensor 2) along the slope direction.

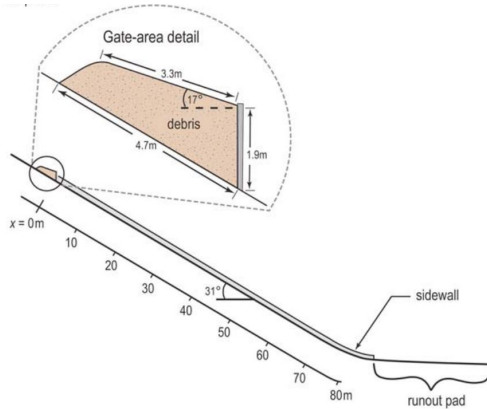


Fig. 1 Flume experimental setup, taken from Iverson et al.

To simulate the experiment, the debris flow was discretized into 1,575 particles with initial spacing of $\Delta x = 0.1$ m. The radius of the support domain is defined as $\kappa h_s = 2.4\Delta x$. To maintain a reasonable amount of neighboring particles during the flow expansion or contraction, an adaptive smoothing length is modified and updated with respect to the initial depth and smoothing length of each

particle. Wall boundary conditions are implemented using fixed virtual fluid particles whose positions and velocities are not evolved through time.

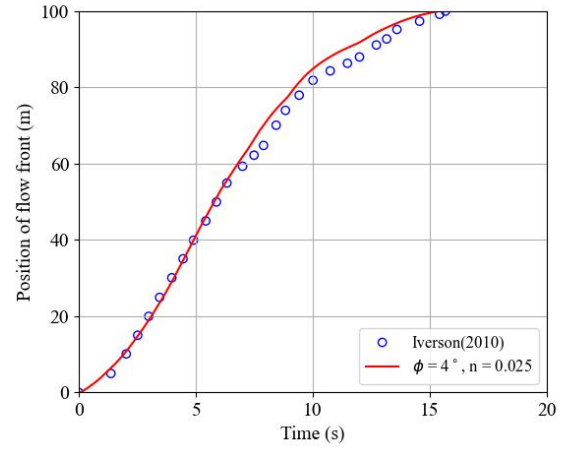


Fig. 2 Propagation of the experimental and simulated flow front in time

Parameter fitting and calibration of the flow resistance parameters, n and ϕ , are conducted to reproduce the results of the experiment. The parameters that best replicated the flow front propagation results are Manning's friction coefficient $n = 0.025$ for the flume floor, and an internal friction angle $\phi = 4^\circ$ (**Fig. 2**). This friction coefficient value corresponds to rough concrete or gravel bottom ($n = 0.025$) consistent with the conditions of the experimental setup, while the friction angle suggests the residual strength of a post-failure mixture of fluidized soil and water.

Another experiment considering the erosion and entrainment of debris flows is also simulated [5]. This time, an erodible sediment bed 12 cm thick is placed spanning from 6 m to 53 m of the channel, while the total debris flow volume is reduced to 6 m³. The experiment then monitors the erosion and channelization due to the debris flow by measuring the elevation changes in the erodible bed. This experiment is simulated using the same calibrated parameters as the previous example. To match the volume, however, the debris flow discretization was reduced to 798 particles. The basal velocity is then assumed to be half of the depth-averaged velocity ($s_1 = 0.5$), and the erodible bed surface is assumed to have an internal friction angle ϕ_s of 40° . Moreover, since the erodible bed material is composed of saturated sediments, a pore pressure ratio 0.5 is assumed. This ratio is used to reduce the effective normal stress acting on the bed surface, defined as the ratio of the pore water pressure to the total normal stress acting on the soil skeleton.

The model is shown to successfully capture the erosion and channelization of the debris flow as it propagates over the erodible bed (**Fig. 3**). Despite the volume being almost half of the previous simulation (11.78 m³ vs 6 m³), the measured flow heights in both simulations are shown

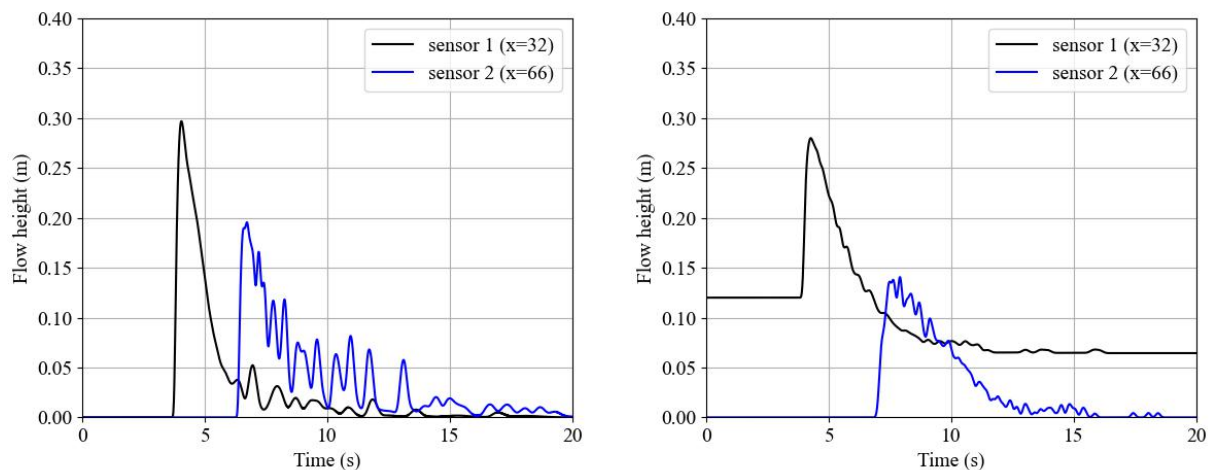


Fig. 3 Simulated debris flow heights as it passes through sensors ($x=32$ m, 66 m) along the channel. The left figure shows the 11.78 m^3 debris flow experiment over the bare non-erodible concrete channel, while the right figure shows the 6 m^3 debris flow experiment over a 12 cm thick erodible bed.

to be relatively more similar than expected, indicating the volume increase due to entrainment of the bed surface. The simulation also depicts the decrease in flow velocities, shown by the gentler drop in flow heights observed in sensor 1. This observation correctly describes the intuitive momentum exchange between an entraining dynamic layer interacting with an eroding static bed surface. Note further the drop in elevation of about 6 cm in the erodible bed right after the flow. These findings highlight the model's potential to represent debris flow dynamics considering entrainment, erosion, and channelization.

The results demonstrate the effectiveness of the adopted depth-integrated shallow water model in simulating debris flows, particularly regarding erosion and entrainment processes. Validation against experimental flume data, first on a non-erodible bed, showcased the model's ability to accurately reproduce flow front propagation by calibrating key resistance parameters like the Manning's friction coefficient and internal friction angle. Moreover, simulation over an erodible bed successfully captured the complex phenomenon of entrainment. The model not only depicted the channelization of the bed surface but also reflected the consequential volume increase of the debris flow due to erosion. Notably, the simulated flow heights in the erodible bed experiment were comparable to those in the non-erodible bed case, despite having a significantly smaller initial volume, directly demonstrating the model's ability to quantify and represent entrainment-driven volume changes.

Further analysis of the erodible bed simulations revealed nuanced dynamic behaviors consistent with physical expectations. The model intuitively reflected the momentum exchange between the flowing debris and the eroding bed, indicated by a decrease in flow velocities. This observation, along with the changes in bed elevation changes after the flow, reinforces the model's capability to simulate the

complex interactions inherent in debris flow entrainment. These findings collectively validate the model as a robust tool for representing key debris flow processes, especially erosion and channelization, and underscore its potential for broader application in geohazard assessments where these processes are critical factors determining the scale and impact of debris flow events.

5. CONCLUSIONS

This study successfully implemented a depth-integrated shallow water model incorporating rheological and entrainment processes using a mesh-free SPH framework. The model was applied to simulate experimental debris flow cases, capturing key dynamic behaviors such as front propagation, flow height evolution, entrainment-induced volume change, and bed surface channelization. Calibration of the flow resistance parameters demonstrated consistency with the physical characteristics of the experimental setup. The results confirm the model's capability to simulate complex debris flow processes, including basal entrainment and channelization. These results highlight the model's capacity to represent key debris flow processes, providing a reliable framework for subsequent application to real-world geohazard scenarios.

REFERENCES

- [1] Iverson, R. M.: Elementary theory of bed-sediment entrainment by debris flows and avalanches., J Geophys Res, 2012.
- [2] Monaghan, J. J.: SPH and Riemann Solvers. J. Comp. Phys., 1997
- [3] Xia, X. et al.: Balancing the source terms in a SPH model for solving shallow water equations. Adv. Water Res., 2013
- [4] Iverson, R. M. et al: The perfect debris flow? aggre-

gated results from 28 largescale experiments. J Geophys Res, 2010.

- [5] Iverson, R. M. et al: Positive feedback and momentum growth during debris-flow entrainment of wet bed sediment. Nature Geoscience, 2011.